Electronic Supplementary Material (ESI) for Journal of Materials Chemistry A.

One-Step Synthesis of Flower-Like Bi_2O_3/Bi_2Se_3 Nanoarchitectures and $NiCoSe_2/Ni_{0.85}Se$ Nanoparticles with Appealing Rate Capability for Constructing High-Energy and Long-Cycle-Life Asymmetric Aqueous Batteries

Alan Meng[a], Xiangcheng Yuan[a], Tong Shen[a], Zhenjiang Li[b#], Qingyan Jiang[c], Hongyao Xue[b], Yusheng Lin[d], Jian Zhao[b*]

[a]*State Key Laboratory Base of Eco-chemical Engineering, College of Chemistry and Molecular Engineering, Qingdao University of Science and Technology, Qingdao 266042, Shandong, P. R. China.*

[b]*Key Laboratory of Polymer Material Advanced Manufacturing Technology of ShandongProvincial,College of Electromechanical Engineering, College of Sino-German Science and Technology, Qingdao University of Science and Technology, Qingdao 266061, Shandong, P. R. China.*

[c]*Ocean College, Zhejiang University, Zhoushan 316021, Zhejiang, P. R. China.*

[d] *College of Materials Science and Engineering, Qingdao University of Science and Technology, Qingdao 266042, Shandong, P. R. China.*

[#]*These authors contributed equally to this work and should be considered co-first authors.*

[*]**Corresponding Author**

E-mail: zhaojian19880105@163.com

Calculations:

(1) The specific capacity (Q) and specific capacitance (C) of the Bi_2O_3/Bi_2Se_3 NFs or $NiCoSe_2/Ni_{0.85}Se$ NPs on graphite substrate electrode calculated from GCD curves are obtained according to the following equation:

$$Q = \frac{I\Delta t}{\Delta V}; C = \frac{I\Delta t}{m\Delta V}$$

where *I* is the discharge current, Δ*t* is the discharge time in GV test, *m* is the active material mass, and Δ*V* is the voltage window.

(2) The specific capacitance of the Bi_2O_3/Bi_2Se_3 NFs//$NiCoSe_2/Ni_{0.85}Se$ NPs asymmetric aqueous battery (AAB) device can be got in accordance with the following equation:

$$C_{device} = \frac{I\Delta t}{M\Delta V}$$

Herein, *I* is the discharge current, Δ*t* is the discharge time in GCD test, *M* is the total mass of both positive and negative electrodes, and Δ*V* is the voltage window of the device.

(3) Methods to calculate the energy and power density of the ASC device:

$$E = \frac{1}{2} C_{device} \Delta V^2 \; ; \; P = \frac{E}{t}$$

Here, C_{device} is the specific capacitance of the device, Δ*V* is the potential window, and *t* is the discharge time.

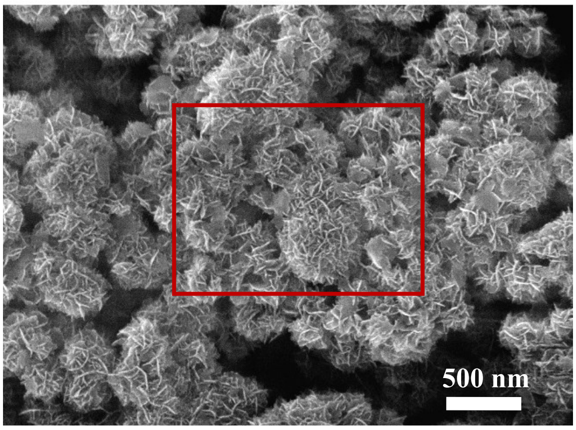

Fig. S1. SEM image of the obtained Bi_2O_3/Bi_2Se_3 NFs.

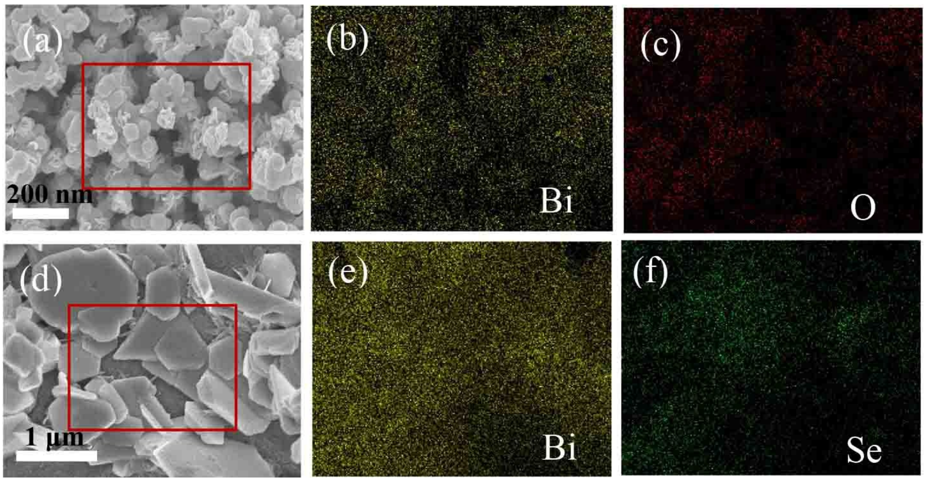

Fig. S2. The elemental mapping of the Bi_2O_3 (a-c) and Bi_2Se_3 sample (d-f).

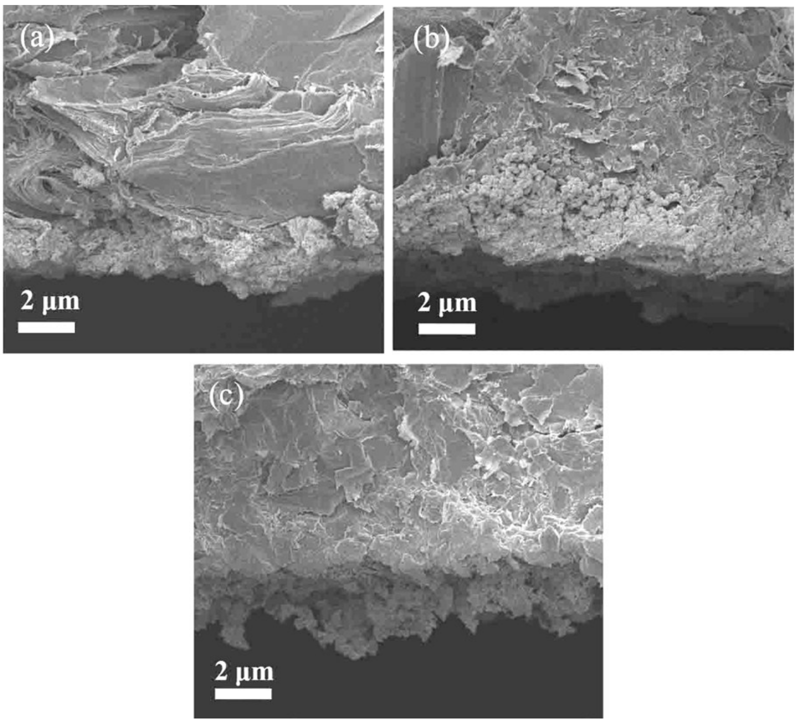

Fig. S3. Low-resolution cross-section SEM images of the Bi_2O_3 (a), Bi_2Se_3 (b) and Bi_2O_3/Bi_2Se_3 (c).

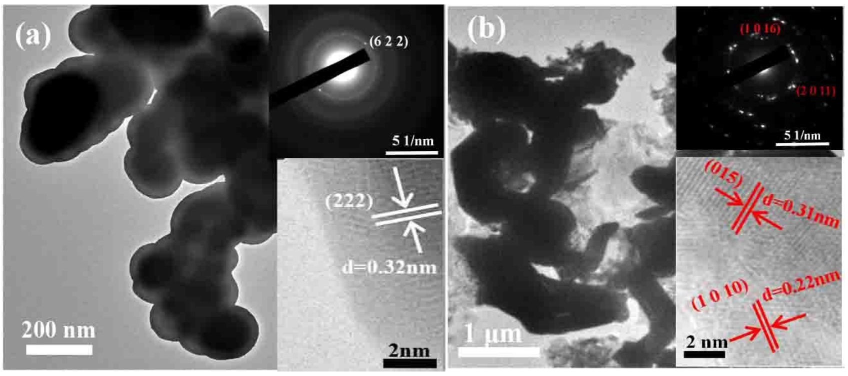

Fig. S4. The typical TEM images of the Bi_2O_3 (a) and Bi_2Se_3 (b) with the insets showing the corresponding SAED patterns and HRTEM images.

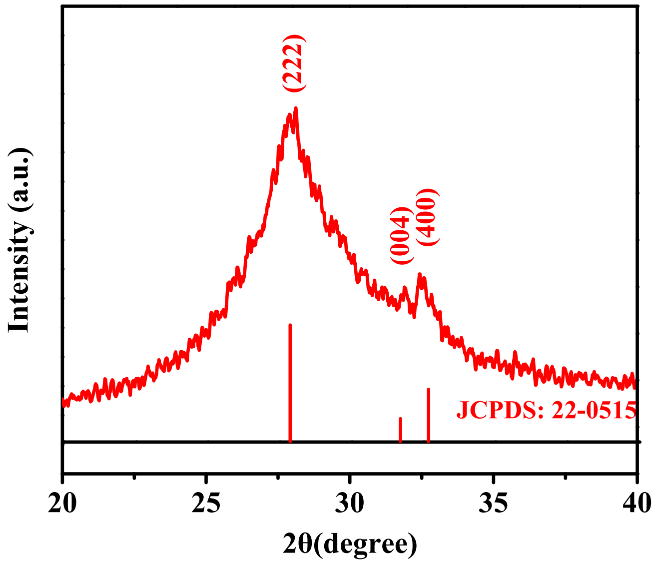

Fig. S5. Local-magnification XRD pattern of Bi_2O_3 NSs.

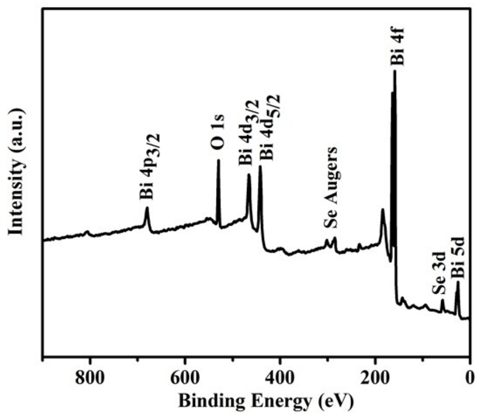

Fig. S6. XPS survey spectrum of Bi_2O_3/Bi_2Se_3 NFs.

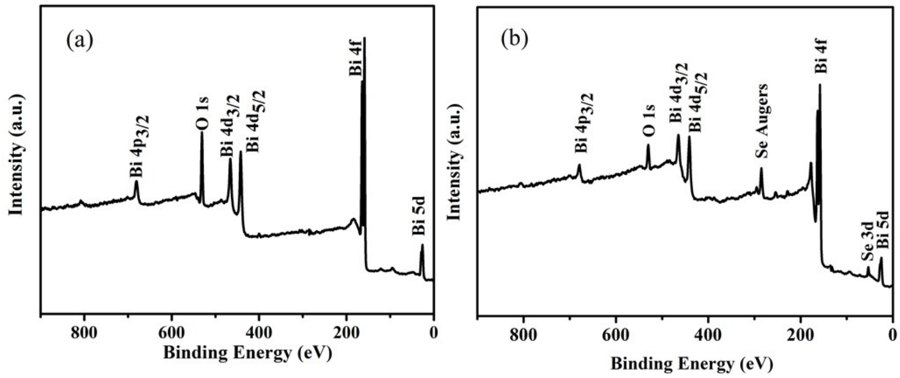

Fig. S7. XPS survey spectrum of the pristine Bi_2O_3 (a) and Bi_2Se_3 (b) products .

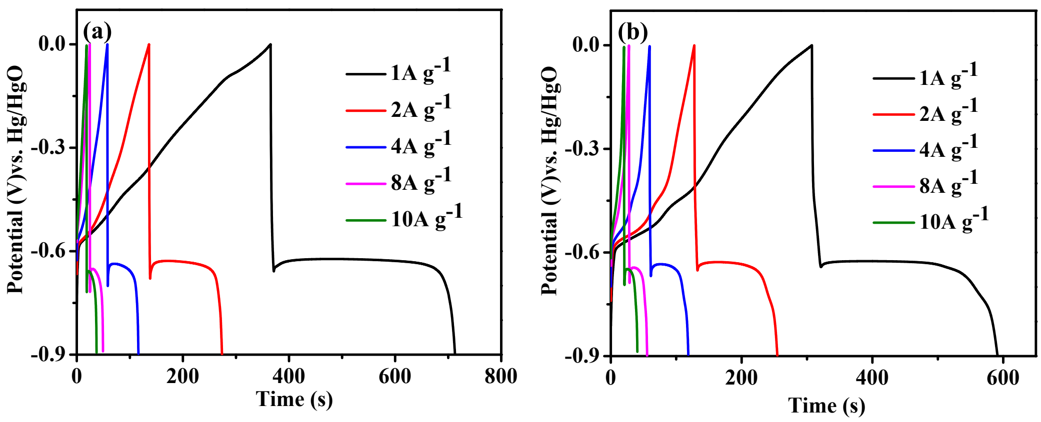

Fig. S8. GCD profiles at different current densities of the Bi_2O_3 NSs (a) and Bi_2Se_3 NSs (b) electrode

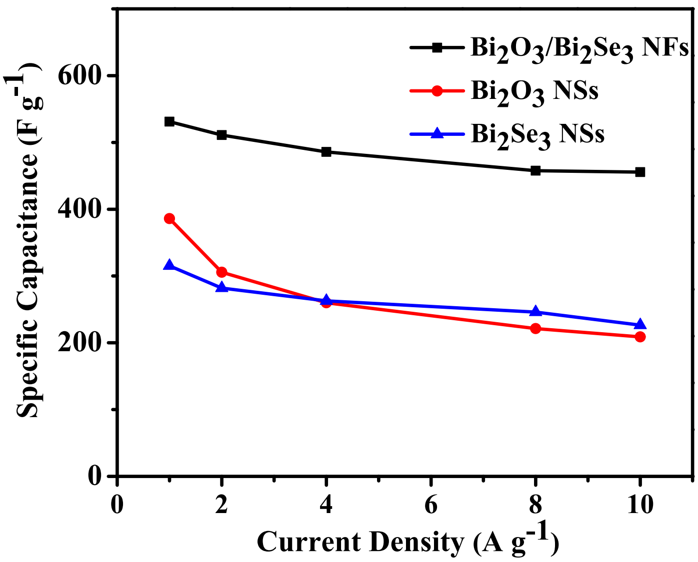

Fig. S9. specific capacitance values of the Bi_2O_3 NSs, Bi_2O_3/Bi_2Se_3 NFs and Bi_2Se_3 NSs electrode versus different current densities

Table S1. Comparison of the electrochemical properties of the Bi_2O_3/Bi_2Se_3 NFs with previously reported negative electrode materials.

Material	Fabrication method	current collector	Specific capacitance or capacity	Rate performance	Reference
Bi_2O_3	Hydrothermal	Ni foam	447 F g^{-1} (2A g^{-1})	260 F g^{-1} (10 A g^{-1})	S1
FeOOH	Electrodeposition	Polyamide Nanofiber Film	315 F g^{-1} (0.5 A g^{-1})	194 F g^{-1} (10 A g^{-1})	S2
Bi_2S_3	Hydrothermal and calcination	S-NCNF	466 F g^{-1} (1 A g^{-1})	299 F g^{-1} (8 A g^{-1})	S3
Bi_2O_3	Room-temperature wet chemical method.	Ni foam	155 mAh g^{-1} (0.4 A g^{-1})	58 mAh g^{-1} (1.8 A g^{-1})	S4
Fe_2O_3	Hydrothermal	Ni foam	158.9 mAh g^{-1} (1 A g^{-1})	32.8 mAh g^{-1} (10 A g^{-1})	S5
WO_3	Calcination	GCE	508 F g^{-1} (1 A g^{-1})	332.2 F g^{-1} (20 A g^{-1})	S6
MoS_2	Hydrothermal	RCF	225 F g^{-1} (0.5A g^{-1})	106 F g^{-1} (5 A g^{-1})	S7
$ZnFe_2O_4$	Calcination	Ni foam	58.7 mAh g^{-1} (1 A g^{-1})	50.2 mAh g^{-1} (1 A g^{-1})	S8
Fe_3O_4	Hydrothermal and calcination	Ni foam	379.8 F g^{-1} (2 A g^{-1})	272.2 F g^{-1} (10 A g^{-1})	S9
Fe_2O_3	Hydrothermal	Ni foam	269 mAh g^{-1} (0.3A g^{-1})	67.3 mAh g^{-1} (12.3 A g^{-1})	S10
Bi_2O_3/Bi_2Se_3	**Solvothermal**	**Graphite substrate**	**132.7 mAh g^{-1} (531F g^{-1}) at 1 A g^{-1}**	**113.8 mAh g^{-1} (455 F g^{-1}) at 10 A g^{-1}**	**In this work**

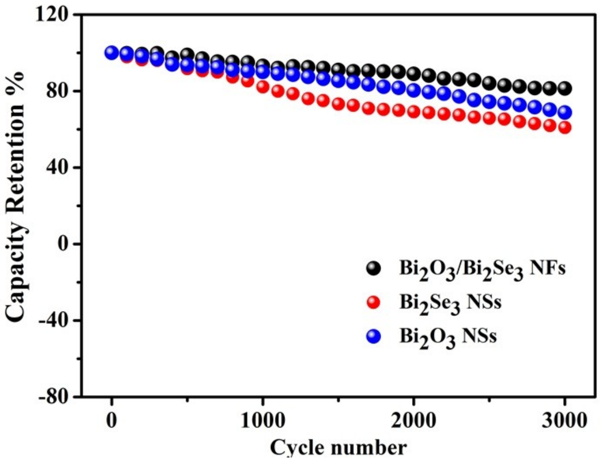

Fig. S10. Cyclic stability of the Bi_2O_3/Bi_2Se_3 NFs Bi_2O_3 NSs and Bi_2Se_3 NSs negative electrode materials over 3000 cycles at 8 A g^{-1}.

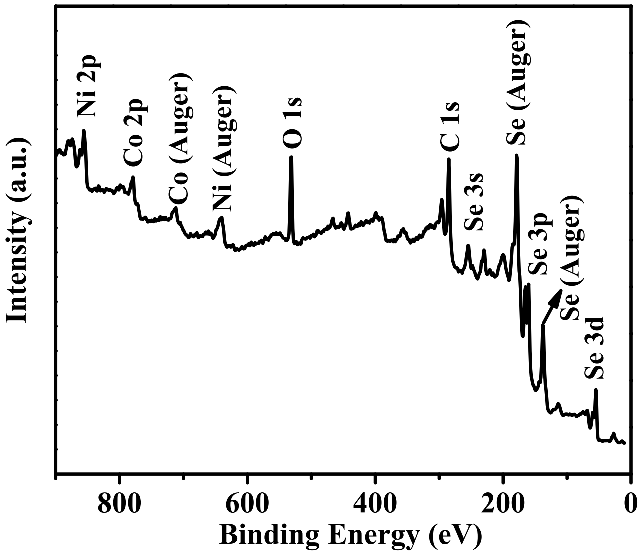

Fig. S11. XPS survey spectrum of the of the $NiCoSe_2/Ni_{0.85}Se$ NPs.

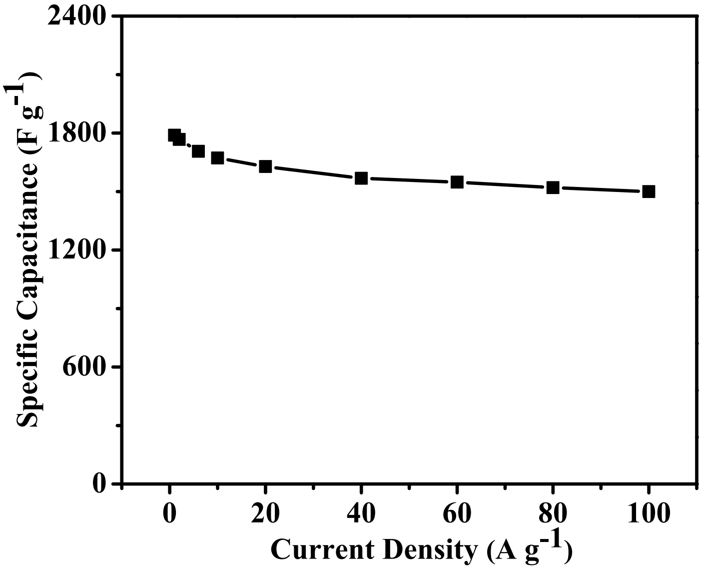

Fig. S12. Specific capacitance of the $NiCoSe_2/Ni_{0.85}Se$ NPs as a function of current densities

Table S2. Electrochemical performances comparison of the $CoNiSe_2/Ni_{0.85}Se$ NPs with other Ni-Co compound based positive electrodes fabricated by different methods.

Material	Fabrication method	current collector	Specific capacitance or capacity	Rate performance	Reference
$(Ni,Co)Se_2$/NiCo-LDH	Calcination and electrodeposition	Carbon substrate	170 mAh g^{-1} (2 A g^{-1})	120.7 mAh g^{-1} (20 A g^{-1})	S11
CoNi-MOF	Hydrothermal and calcination	Ni foam	1044 F g^{-1} (2 A g^{-1})	569 F g^{-1} (32A g^{-1})	S12
$CoNi_2S_4$	Chemical deposition	Ni foam	1530 F g^{-1} (1 A g^{-1})	1346 F g^{-1} (8 A g^{-1})	S13
$NiCo_2O_4$/CNT	Calcination	Ni foam	1596 F g^{-1} (1 A g^{-1})	1406 F g^{-1} (10 A g^{-1})	S14
Ni_3S_2	Hydrothermal	Ni foam	70 mAh g^{-1} (2mA cm^{-2})	------------	S15
$CoNiSe_2$	Solvothermal and calcination	Ni foam	750 F g^{-1} (1 A g^{-1})	660 F g^{-1} (20 A g^{-1})	S16
$NiSe_2$	Plasma-exfoliation	Ni foam	466 F g^{-1} (3 A g^{-1})	328 F g^{-1} (20 A g^{-1})	S17
$NiCo_2O_4$	Hydrothermal and calcination	Carbon cloth	1055 F g^{-1} (0.4 A g^{-1})	483 F g^{-1} (10 A g^{-1})	S18
Co_3O_4/Ni-based MOFs	Hydrothermal	Carbon cloth	209 mAh g^{-1} (2 A g^{-1})	~58 mAh g^{-1} (10 A g^{-1})	S19
$Co_3O_4/Co(OH)_2$	Hydrothermal	polyethylene naphthalate	184.9 mAh g^{-1}(1 A g^{-1})	129.4 mAh g^{-1} (16 A g^{-1})	S20
$NiCoSe_2/Ni_{0.85}Se$	**Electrodeposition**	**Graphite substrate**	**248.4 mAh g^{-1} (1788 F g^{-1}) at 1 A g^{-1}**	**208 mAh g^{-1} (1500 F g^{-1}) at 100A g^{-1}**	**In this work**

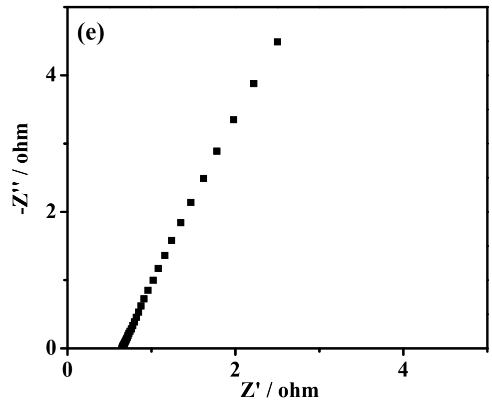

Fig. S13. Nyquist plot of the $NiCoSe_2/Ni_{0.85}Se$ NPs hybrid electrode.

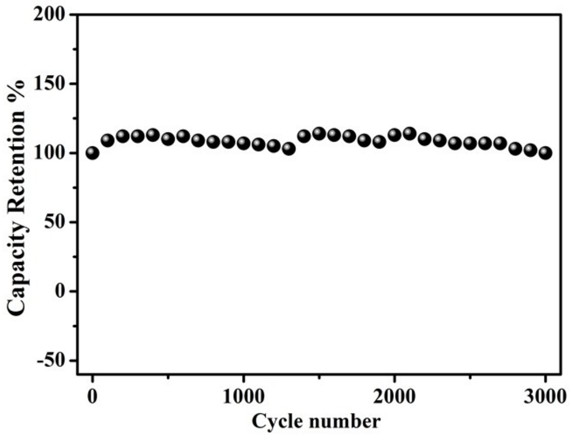

Fig. S14. Cyclic stability of the $NiCoSe_2/Ni_{0.85}Se$ NPs hybrid positive electrode materials over 3000 cycles at 10 A g^{-1}.

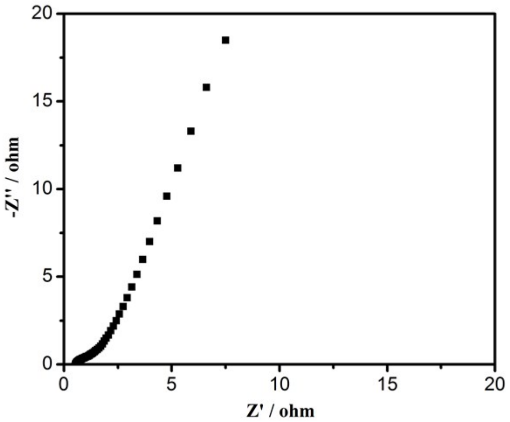

Fig. S15. The Nyquist plot of the device.

Table. S3 Cycle performance comparison of the assembled AAB with other state-of-the-art devices with various positive and negative electrodes.

ASC devices	Cell voltage (V)	Cycle performance	Reference
Fe_2O_3-P//MnO_2	1.6	88% retention after 9000 cycles	S21
MnO_2//Fe_2O_3	2.2	83% retention after 3000 cycles	S22
Co_3O_4//γ-Fe_2O_3	1.7	80.1% retention after 5000 cycles	S23
Ni-Co-S-W/NF//AC/NF	1.8	91.7% retention after 6000 cycles	S24
MnO_2/CNT//CNT/PPy	1.5	80% retention after 5000 cycles	S25
Ni-Co-N/GP//GOP	1.5	95% retention after 5000 cycles	S26
NF@NiO//FeOOH HSCs	1.7	84.7% retention after10000 cycles	S27
ZnNiCo-P//PPD-rGOs	1.6	89% retention after 8000 cycles	S28
NiO–CuO//PGH	1.6	90.4% retention after 5000 cycles	S29
CC/H-Ni@Al-Co-S//graphene/CNT	1.8	90.6% retention after 10000 cycles	S30
Bi_2O_3/Bi_2Se_3//$NiCoSe_2$/$Ni_{0.85}Se$	**1.6**	**91.5% retention after 10000 cycles**	**In this work**

References

S1 N. Shinde, Q. Xia, J. Yun, R. Mane and K. Kim, *Acs Appl. Mater. Interfaces*, 2018, **10**, 11037.

S2 T. Gao, Z. Zhou, J. Yu, D. Cao, G. Wang, B. Ding and Y. Li, *ACS appl. mater. Interfaces*, 2018, **10**, 23834.

S3 W. Zong, F. Lai, G. He, J. Feng, W. Wang, R. Lian, Y. Miao, G. Wang, I. Parkin and T. Liu, *Small*, 2018, **14**, 1801562.

S4 N. Shinde, Q. Xia, J. Yun, P. Shinde, S. Shaikh, R. Sahoo, S. Mathur, R. Mane and K. Kim, *Electrochim. Acta*, 2019, **296,** 308.

S5 X. Yun, J. Li, Z. Luo, J.Tang and Y. Zhu, *Electrochim. Acta*, 2019, **302**, 449.

S6 D. Mandal, P. Routh and A. K. Nandi, *Small*, 2018, **14**, 1702881.

S7 C. Zhao, Y. Zhou, Z. Ge, C. Zhao and X. Qian, *Carbon*, 2018, **127**, 699.

S8 Yang, Z. Han, F. Zheng, J. Sun, Z. Qiao, X. Yang, L. Li, C. Li, X. Song and B. Cao, *Carbon*, 2018, **134**, 15.

S9 F. Li, H. Chen, X. Liu, S. Zhu, J. Jia, C.. Xu, F. Dong, Z. Wen and Y. Zhang, *J. Mater. Chem. A*, 2016, **4**, 2096.

S10 J. Zhu, L. Li, Z. Xiong, Y. Hu and J. Jiang, *ACS Sustainable Chem. Eng.*, 2017, **5**, 269.

S11 X. Li, H. Wu, C. Guan, A. Elshahawy, Y. Dong, S. Pennycook and J. Wang, *Small*, 2019, **15**, 1803895.

S12 T. Deng, Y. Lu, W. Zhang, M. Sui, X. Shi, D. Wang and W. Zheng, *Adv. Energy Mater.*, 2018, **8**, 1702294.

S13 X. Cao, J. He, H. Li, L. Kang, X. He, J. Sun, R. Jiang, H. Xu, Z. Lei and Z. Liu, *Small*, 2018, **14**, 1800998.

S14 P. Wu, S. Cheng, M. Yao, L. Yang, Y. Zhu, P. Liu, O. Xing, J. Zhou, M. Wang and H. Luo, *Adv. Funct. Mater.*, 2017, **27**, 1702160.

S15 K. Tao, Y. Gong, Q. Zhou and J. Lin, *Electrochim. Acta*, 2018, **286**, 65.

S16 L. Hou, Y. Shi, C. Wu, Y. Zhang, Y. Ma, X. Sun, J. Sun, X. Zhang and C. Yuan, *Adv. Funct. Mater.*, 2018, **28**, 1705921.

S17 A. Chang, C. Zhang, Y. Yu, Y. Yu and B. Zhang, *ACS appl. mater. Interfaces*, 2018, **10**, 41861.

S18 C. Guan, X. Liu, W. Ren, X. Li, C. Cheng and J. Wang, *Adv. Energy Mater.*, 2017, **7**, 1602391.

S19 L. Zhang, Y. Zhang, S. Huang, Y. Yuan, H. Li ,Z. Jin , J. Wu, Q. Liao, L. Hu, J. Lu, S. Ruan and Y. Zeng, *Electrochim. Acta*, 2018, **281**, 189.

S20 G. Lee and J. Jang, *J. Power Sources*, 2019, **423**, 115.

S21 H. Liang, C. Xia, A. Emwas, D. Anjum, X. Miao and H. Alshareef, *Nano energy*, 2018, **49**, 155.

S22 M. Zhang, Y. Li and Z. Shen, *J. Power Sources*, 2019, **414**, 479.

S23 R. Wang, Y. Sui, S. Huang, Y. Pu and P. Cao, *Chem. Eng. J.*, 2018, **331**, 527.

S24 W. He, Z. Liang, K. Ji, Q. Sun, T. Zhai and X. Xu, *Nano Res*., 2018, **11**, 1415.

S25 J. Yu, W. Lu, J. Smith, K. Booksh, L. Meng, Y. Huang, Q. Li, J. Byun, Y. Oh and Y. Yan, *Adv. Energy Mater*., 2017, **7**, 1600976.

S26 F. Liu, L. Zeng, Y. Chen, R. Zhang, R. Yang, J. Pang, L. Ding, H. Liu and W. Zhou, *Nano Energy*, 2019, **61**, 18.

S27 Q. Chen, J. Li, C. Liao, G. Hu, Y. Fu, O. K. Asare, S. Shi, Z. Liu, L. Zhou and L.

Mai, *J. Mater. Chem. A*, 2018, **6**, 19488.

S28 J. Li, Z. Liu, Q. Zhang, Y. Cheng, B. Zhao, S. Dai, H.-H. Wu, K. Zhang, D. Ding and Y. Wu, *Nano Energy*, 2019, **57**, 22.

S29 Z. Fang, S. ur Rehman, M. Sun, Y. Yuan, S. Jin and H. Bi, *J. Mater. Chem. A*, 2018, **6**, 21131.

S30 J. Huang, J. Wei, Y. Xiao, Y. Xu, Y. Xiao, Y. Wang, L. Tan, K. Yuan and Y. Chen, *ACS nano*, 2018, **12**, 3030.